Beam scanning coherent Fourier scatterometry

Soman, S.; Pereira, S.F.

DOI
10.1117/12.3022937

Publication date
2024

Document Version
Final published version

Published in
Optical Instrument Science, Technology, and Applications III

Citation (APA)
Soman, S., & Pereira, S. F. (2024). Beam scanning coherent Fourier scatterometry. In H. Münz, B. N. Sitarski, & R. N. Youngworth (Eds.), *Optical Instrument Science, Technology, and Applications III* Article 1302408 (Proceedings of SPIE - The International Society for Optical Engineering; Vol. 13024). SPIE. https://doi.org/10.1117/12.3022937

Beam scanning coherent Fourier scatterometry

S. Soman*, S. F. Pereira
Department of Imaging Physics, Faculty of Applied Sciences, Delft University of Technology,
Lorentzweg 1, 2628 CJ Delft, The Netherlands

ABSTRACT

The significance of precise metrology in various industries, particularly within manufacturing plants, is undeniable, especially as components and devices continue to undergo miniaturization. The emergence of nano-manufacturing further amplifies the necessity for meticulous measurement techniques. Coherent Fourier scatterometry (CFS) is a non-imaging, model-based, bright-field optical metrology and inspection technique used for retrieving complex geometric parameters of nanostructures and for detecting isolated nanoparticles and contamination on surfaces. It uses a focused light spot to illuminate the sample and the scattered light is collected as the sample is scanned in the lateral direction. However, the time it takes to inspect a certain area has been a limiting factor in its wider adoption as a commercial metrology tool. To address this limitation, we propose a novel design of CFS utilizing a galvo mirror for faster scanning of the laser spot on the sample, offering significant improvements in scan speed.

Keywords: Scatterometry, optical metrology, scanning, contamination inspection

INTRODUCTION

Metrology, as the engineering discipline dedicated to precise measurement, holds a pivotal role across various industries, notably evident within manufacturing plants. As components and devices continue to undergo miniaturization, the field of nanomanufacturing becomes increasingly vital [1]. Future nano-systems integrating electrical, optical, magnetic, mechanical, chemical, and biological devices demand precise metrology for critical parameters such as structure dimensions, surface smoothness, defect detection, and more, with dimensional control being particularly crucial for ensuring manufacturability and performance consistency [2]. The inherent correlation between the small size of nanostructures and their functional properties underscores the criticality of dimensional precision. Any deviation from the intended dimensions can result in significant variations in performance, compromising the functionality and reliability of the nano-systems.

Scatterometry is a non-imaging, model-based optical metrology technique used to retrieve the complex parameters of nanostructures [3]. It uses the scattered light from a surface as a function of incident angle or wavelength. Compared to traditional metrology tools such as scanning electron microscopy (SEM) or atomic force microscopy (AFM), scatterometry techniques are non-contact, non-destructive and do not require stringent measurement conditions. Coherent Fourier scatterometry is an advanced scatterometry technique in which the response to multiple angles of incidence is recorded simultaneously by capturing the Fourier plane using a detector [4]. The probe consists of a laser beam which is focused on the sample surface using an objective lens. The light after reflection is captured by the same objective and relayed to the detector. The small size of the probe, namely, the focused spot, implies the sample to be scanned in two directions to cover the entire surface. A major limitation of the technique is the time it takes to scan a certain area of the sample. Thus, the method is inherently limited by the scanning speed of the setup and it is crucial to improve this aspect to facilitate its wider adoption as a commercial metrology tool for applications in contamination detection in large areas.

In the previous iterations of the system, the sample was raster scanned using a piezo-based translator. These translators, while having sub-nanometer precision are slow. Here we propose a new design using a galvo mirror to scan the surface in the fast-axis. Galvo mirrors have long been used in a wide range of avenues such as different microscopy techniques for imaging purposes, LIDAR systems, optical coherence tomography, laser cutting and so on [5-8]. We make use of a single axis galvo mirror to both scan and rescan the beam such that the beam at the detector is static. In the following sections we discuss the experimental setup and design caveats, the scan speed improvements and calibration measurements.

*s.soman@tudelft.nl

Optical Instrument Science, Technology, and Applications III, edited by Holger Münz,
Breann N. Sitarski, Richard N. Youngworth, Proc. of SPIE Vol. 13024,
1302408 · © 2024 SPIE · 0277-786X · doi: 10.1117/12.3022937

EXPERIMENTAL SETUP

The schematic of the setup is shown in Figure 1. Lenses L1 (f = 10 mm) and L2 (f = 250 mm) were used to expand light from a 633 nm, He Ne laser, to the galvo mirror, M2. A 1 kHz single-axis galvo mirror (GVS211/M, Thorlabs) was chosen for the beam scanning. The mirror is placed at the back focal plane of lens L3 (LSM03-VIS, Thorlabs) to ensure that the beam after reflection from the sample is not shifted with respect to the incident beam. The beam from M2 is relayed to the back focal plane of the objective using lenses L3 and L4 (TTL165-A). The beam was focused on the sample using 0.4 NA (Leica, N PLAN L 20x/0,40) objective. The beam after reflection from the sample is captured by the same objective and relayed to the detector after demagnification using lenses L5 (f = 275 mm) and L6 (f = 40 mm). The beam after demagnification is incident in the middle of the detector. Lenses L5 and L7 (f = 100 mm) are also in a telescopic arrangement to demagnify the beam and relay the Fourier plane to the camera. M3, a flipping mirror, is used to switch between the detector and camera arm. The camera (Microsoft LifeCam Cinema) is used to locate areas of interest in the sample. Reference mirror M4 is used to ensure that the sample is in focus. A piezo translator (P-625.2 CD) is used to scan the sample in the slow axis. An additional z-stage (S-316.10H) is used to position the sample in the focal plane of the objective.

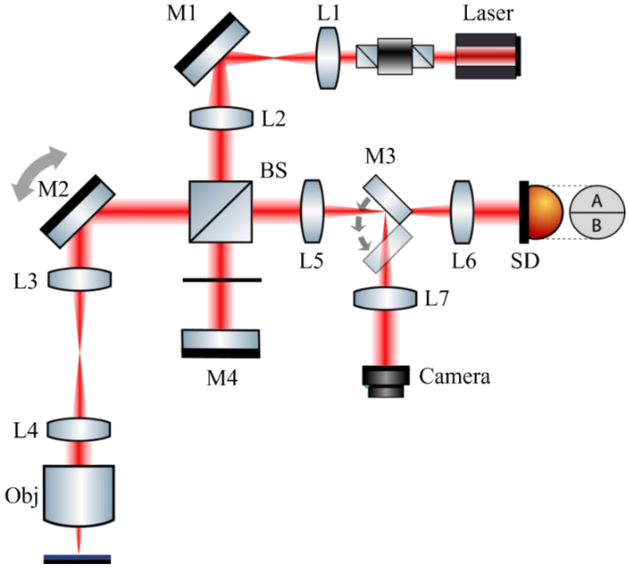

Figure 1. Schematic of the optical setup. Lenses: L1-L7, BS: beam splitter, mirrors: M1-M4, Obj: 0.4 NA objective, SD: split detector. Galvo mirror (M2), camera and the split-detector are in the Fourier plane of the sample.

The detector consists of a pair of photodiodes (SD113-24-21-021) working as a balanced/split detector. When light is incident on each photodiode a photocurrent proportional to the intensity of the incident light is generated. The current from one photodiode is subtracted from the other to generate the output difference signal. The detector is aligned such that the beam is incident on the split detector exactly in the middle of the two diodes. The output signal is zero when the beam is symmetrical but becomes non-zero when scanning across a scattering object which creates an asymmetrical far field. The use of the difference signal eliminates common mode noise. The signal is then amplified using a multi-stage amplifier and sampled using a 16-bit ADC (NI 5734). The output is further represented as a 2D dataset using the feedback signals from both the piezo and the galvo mirror.

Effect of galvo mirror position

As mentioned briefly in the description of the experimental setup, the galvo mirror is placed in the exit pupil of the system. Following geometrical optics, this would mean that the chief ray would be parallel to the optical axis after being focused by the objective on the sample and after reflection it would follow the same path to the mirror for all scan angles. If the mirror is shifted from the exit pupil, the chief ray is no longer parallel to the optical axis and after the second pass through the mirror arm it is shifted laterally. The shift can be calculated using trigonometric relations as shown by Carlsson [9].

This lateral shift has two problems: vignetting in the images and the shift of the incident beam at the detector. The former can be reduced by having a larger input beam diameter compared to the pupil size at the cost of poor use of laser power. The latter generates an output signal baseline oscillating with the same frequency as that of the mirror and amplitude proportional to the shift of the galvo mirror from the exit pupil. It is possible to filter the baseline frequency during post-processing since the driving frequency of the mirror is known in advance.

RESULTS

Before using the galvo mirror for beam scanning, the response of the mirror at different input frequencies and voltages was studied. The input voltage signals were generated using an external function generator and had the general form, $V_{in} = V_{pp} \sin(2\pi f t + \varphi) + V_{offset}$. The calibration curves are presented in Figures 2 and 3. Figure 2 shows the frequency response of the galvo at different voltages and vice versa. From Figure 2.b, it is evident that the mirror response flattens at higher frequencies. This has to be taken into account to be able to scan the same area at different frequencies. Figure 3 shows the beam angle as a function of the input voltage. The slope is calculated to be 0.253 ± 0.004 V/degree. Note that the beam angle is double that of the mirror angle and matches the nominal scaling factor of 0.5 V/degree quite well.

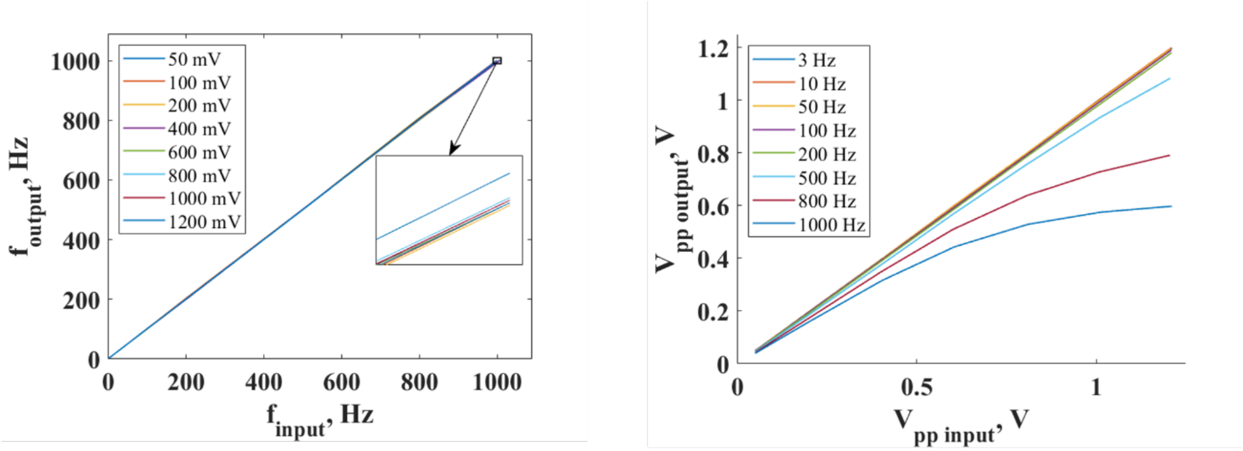

(a) (b)

Figure 2. Galvo response to different input frequencies and voltages.

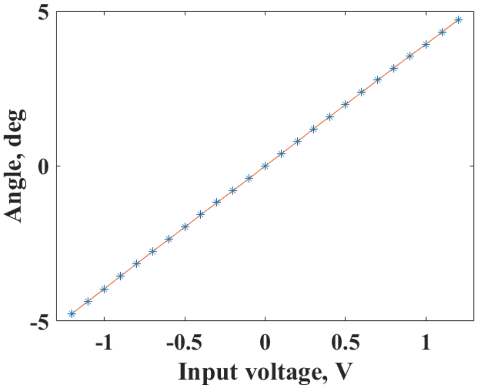

Figure 3. Beam angle as a function of input voltage

The effect of the lateral shift of the beam due to the position of the mirror with respect to the exit pupil on the output signal is shown in Figure 4.

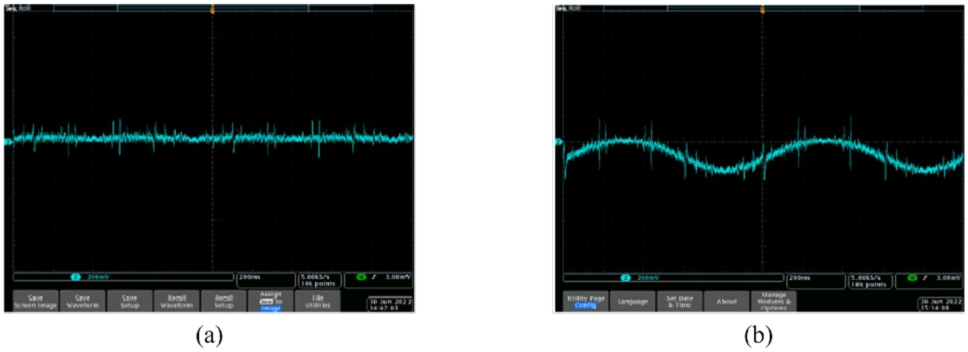

(a) (b)

Figure 4. The split detector signal when galvo mirror a) coincides with and b) is shifted by 5 mm with respect to the exit pupil position. The signal from the sample surface is overlaid on top of the signal due to the beam displacement.

Using the feedback signal from the mirror the data acquired can be visualized as a 2D plot. This is shown in Figure 5. The scan sample consists of an array of holes etched in Si wafer. The diameter of the holes varies from 25 nm to 1125 nm in steps of 50 nm. The etch depth is 166 nm. The scan parameters were: 200 um x 126.7 um scan area, 100 Hz galvo frequency, 800 mVpp input voltage, 200 nm separation between each line, 633 nm incident light wavelength, 69 uW laser power at the sample, and 0.4 NA objective. The signal was sampled at a 1MHz sampling rate. The total time taken to scan the area was 10 seconds. For comparison, the time taken to scan the same area using the piezo stage (P-625.2 CD) is 800 seconds using a speed of about 0.31 mm/s.

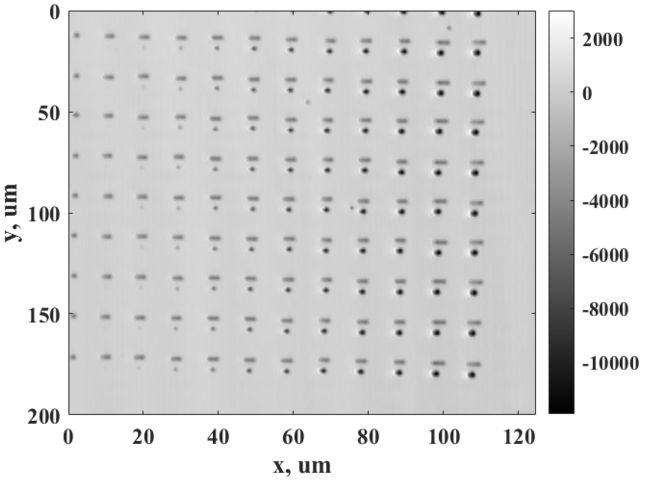

Figure 5. CFS scan using galvo mirror visualized as a 2D plot using feedback signal. The scan sample consists of an array of etched holes in a Si wafer. Within each row, the diameter varies from 25 nm to 1125 nm in steps of 50 nm. The etch depth is 166 nm.

DISCUSSIONS

In summary, we have presented a beam-scanning coherent Fourier scatterometer using a single-axis galvo mirror. The design places the rotational axis of the mirror in the exit pupil of the objective such that the beam is rescanned by the same mirror before it goes to the detector. This ensures that there is no angle-dependent beam shift. The galvo mirror response at different frequencies and voltages was characterized before its use in the setup. In the slow axis, the sample is scanned using a piezo stage. It is possible to use a dual-axis galvo mirror to completely replace the sample stage. The caveat would be that the rotational axis still has to be in a plane conjugated with the exit pupil plane. In the current example, we demonstrated a scan time improvement of 80x compared to the previous versions using a piezo stage. However, the scan speed in principle can be improved further using a high-bandwidth detector. This would in turn come at the expense of additional laser power to maintain a similar signal-to-noise ratio. A possible limitation of the current design is the signal distortion at higher angles due to the field curvature. The scan area is limited by the field of view of the objective used.

ACKNOWLEDGEMENTS

The authors acknowledge Roland Horsten and Thomas Scholte of Delft University of Technology for the electronics and the mechanical works. We also acknowledge the Nederlandse Organisatie voor Wetenschappelijk Onderzoek (Project 17-24 Synoptics No. 2) for funding this research.

REFERENCES

[1] F. Fang, X. Zhang, W. Gao, Y. Gao, G. Byrne and H. Hansen, "Nanomanufacturing—Perspective and applications," *CIRP Annals,* vol. 66, no. 2, pp. 683-7-5, 2017.

[2] M. L. Schattenbur and H. I. Smith, "The critical role of metrology in nanotechnology," *Proceedings Volume 4608, Nanostructure Science, Metrology, and Technology,* 2002.

[3] M. H. Madsen and P.-E. Hansen, "Scatterometry—fast and robust measurements of nano-textured surfaces," *Surface Topography: Metrology and Properties,* vol. 4, p. 023003, 2016.

[4] S. Roy, A. C. Assafrão, S. F. Pereira and H. P. Urbach, "Coherent Fourier scatterometry for detection of nanometer-sized particles on a planar substrate surface," *Opt. Express ,* vol. 22, pp. 13250-13262, 2014.

[5] J. B. Pawley, Handbook of Biological Confocal Microscopy, Springer New York, NY, 2006.

[6] X. T. Nguyen, V. L. Dinh and H. J. L. a. H. Kim, "A High-Definition LIDAR System Based on Two-Mirror Deflection Scanners," *IEEE Sensors Journal,* vol. 18, no. 2, pp. 559-568, 2018.

[7] V.-F. Duma, K.-s. Lee, P. Meemon and J. P. Rolland, "Experimental investigations of the scanning functions of galvanometer-based scanners with applications in OCT," *Applied Optics,* vol. 50, no. 29, pp. 5735-5749, 2011.

[8] C. Leone, S. Genna and V. Tagliaferri, "Fibre laser cutting of CFRP thin sheets by multi-passes scan technique," *Optics and Lasers in Engineering,* vol. 53, pp. 43-50, 2014.

[9] K. Carlsson, "Scanning and detection techniques used in a confocal," *Journal of microscopy,* vol. 157, pp. 21-27, 1989.